Effective Date: June 19, 2014
Revision B

GSFC JPSS CMO
September 22, 2014
Released

Joint Polar Satellite System (JPSS) Ground Project
Code 474
474-00028

Joint Polar Satellite System (JPSS) VIIRS Earth Gridding Algorithm Theoretical Basis Document (ATBD)

For Public Release

The information provided herein does not contain technical data as defined in the International Traffic in Arms Regulations (ITAR) 22 CFC 120.10. This document has been approved For Public Release to the NOAA Comprehensive Large Array-data Stewardship System (CLASS).

National Aeronautics and Space Administration

Goddard Space Flight Center
Greenbelt, Maryland

Joint Polar Satellite System (JPSS)

VIIRS Earth Gridding

Algorithm Theoretical Basis Document (ATBD)

JPSS Electronic Signature Page

Prepared By:

Ray Godin, EDR Lead
JPSS Data Products and Algorithms
(Electronic Approvals available online at https://jpssmis.gsfc.nasa.gov/mainmenu_dsp.cfm)

Approved By:

Eric Gottshall
JPSS Data Products and Algorithms Manager

(Electronic Approvals available online at https://jpssmis.gsfc.nasa.gov/mainmenu_dsp.cfm)

Goddard Space Flight Center

Greenbelt, Maryland

Preface

This document is under JPSS Ground configuration control. Once this document is approved, JPSS approved changes are handled in accordance with Class I and Class II change control requirements as described in the JPSS Configuration Management Procedures, and changes to this document shall be made by complete revision.

Any questions should be addressed to:

JPSS Configuration Management Office
NASA/GSFC
Code 474
Greenbelt, MD 20771

Change History Log

Revision	Effective Date	Description of Changes (Reference the CCR & CCB/ERB Approve Date)
Original	04/22/2011	**474-CCR-11-0043**: This version baselines D43778, VIIRS Earth Gridding Algorithm Theoretical Basis Document ATBD (ref Y7051), Rev A dated 12/03/2008 as a JPSS document, version Rev –. This is the version that was approved for NPP launch. Per NPOESS CDFCB - External, Volume V – Metadata, doc number D34862-05, this has been approved for Public Release into CLASS. This CCR was approved by the JPSS Algorithm ERB on April 22, 2011.
A	09/18/2013	**474-CCR-13-1078**: Approved by the JPSS Algorithm ERB on September 18, 2013. Section 4.3.4.1 was changed.
B	06/19/2014	**474-CCR-13-1043**: Approved by the JPSS Algorithm ERB on June 19, 2014. Table 2 and Section 4.3.4.10 were changed.

Northrop Grumman Space & Mission Systems Corp.
Space Technology
One Space Park
Redondo Beach, CA 90278

Engineering & Manufacturing Development (EMD) Phase
Acquisition & Operations Contract

CAGE NO. 11982

VIIRS Earth Gridding Algorithm Theoretical Basis Document ATBD (ref Y7051) CDRL A032

Document Number: D43778

Document Date:12/03/2008 **Revision: A**

Point of Contact: Alain Sei, Algorithms, Models & Simulations

ELECTRONIC APPROVAL SIGNATURES:

Merit Shoucri, Algorithms, Models & Simulations Lead

Prepared by
Northrop Grumman Space Technology
One Space Park
Redondo Beach, CA 90278

Prepared for
Department of the Air Force
NPOESS Integrated Program Office
C/O SMC/CIK
2420 Vela Way, Suite 1467-A8
Los Angeles AFB, CA 90245-4659

Under
Contract No. F04701-02-C-0502

DISTRIBUTION STATEMENT F: Distribution statement "F" signifies that further dissemination should only be made as directed by the controlling DoD Office (NPOESS IPO). Ref DODD 5230.24D.

Northrop Grumman Space & Mission Systems Corp.
Space Technology
One Space Park
Redondo Beach, CA 90278

Revision/Change Record

Document Number D43778

Revision	Document Date	Revision/Change Description	Pages Affected
---	02/06/2007	Initial PCIM Release to bring document into Matrix Accountability. Reference original document number: Y7051 delivered in 2004	All
A	12/03/2008	Changes due to RFA for CDA ECR A 204. Corrected typos and changed references to Integerized Sinusoidal grid to Sinusoidal grid	iii-ix, 2, 9, 11-14, 16, 24-28, 30, 32-35, 40

Revision	Document Date	Revision/Change Description	Pages Affected
4r0	March, 2002	See Section 1.4	Unknown
5r0	January, 2002	See Section 1.4	See Section 1.4
5r1	February 11, 2004	See Discussion in Section 1.4.	All
5r2	April, 2004	See Discussion in Section 1.4.	All
5r3	July 14, 2004	Added discussion of Area Weighting.	Section 4.3.3.4
5r4	17 September 2004	Changes to NN and AW discussions. Cleaned up Glossary of Acronyms. SPCR#: ALG00000554.	All

TABLE OF CONTENTS

Page

LIST OF FIGURES

LIST OF TABLES

Page

GLOSSARY OF ACRONYMS

ATBD	Algorithm Theoretical Basis Document
API	Application Programming Interface
BRDF	Bi-directional Reflectance Distribution Function
CDR	Critical Design Review
CrIS	Cross-track Infrared Sounder
DEM	Digital Elevation Model
DPA	Data Processing Architecture
DoD	Department of Defense
ECS	EOSDIS Core System
EDR	Environmental Data Record
EOSDIS	Earth Observing System Data and Information System
GCTP	General Cartographic Transformation Package
GDSR	Gridded Daily Surface Reflectance
GMBT	Gridded Monthly Brightness Temperature
GMSR	Gridded Monthly Surface Reflectance
GMVI	Gridded Monthly Vegetation Index
GSD	Ground Sample Distance
GSIC	Gridded Snow/Ice Cover
GWN	Greatest Weight Neighbor
HDF-EOS	Hierarchical Data Format-Earth Observing System
HSI	Horizontal Sampling Interval
HSR	Horizontal Spatial Resolution
IP	Intermediate Product
MNSR	Monthly Non-snow Surface Reflectance
MODIS	Moderate-Resolution Imaging Spectroradiometer
NASA	National Aeronautics and Space Administration
NCEP	National Center for Environmental Predication
NDVI	Normalized Difference Vegetation Index
NOAA	National Oceanic and Atmospheric Administration
NPOESS	National Polar-orbiting Operational Environmental Satellite System
NPP	Net Primary Productivity
OMPS	Ozone Mapping and Profiler Suite
SBRS	Santa Barbara Remote Sensing
SDR	Sensor Data Record

SNR	Signal-to-Noise Ratio
TOA	Top of Atmosphere
TOC	Top of Canopy
USGS	United States Geological Survey
VIIRS	Visible/Infrared Imager/Radiometer Suite
VVI	VIIRS Vegetation Index

ABSTRACT

During the National Polar-orbiting Operational Environmental Satellite System (NPOESS) mission, Environmental Data Records (EDRs) will be produced operationally by running a variety of retrieval algorithms through the NPOESS ground processing system, the Interface Data Processing Segment (IDPS). Many of the retrieval algorithms require input data obtained from sources external to a specific sensor swath. External data sources include non-NPOESS sources (e.g., NCEP), data from other NPOESS sensors, and data from previous swaths of the same sensor. To be able to match the external data to the correct sensor swath data, a means of co-locating the data must be used. The approaches used to accomplish this are organized under the general term “gridding/re-gridding”, because the most common methods involve mapping swath data to a fixed external grid (gridding) and the inverse process of mapping external gridded data to the sensor swath (re-gridding). This ATBD describes the methods that will be implemented to accomplish gridding and re-gridding of data used by the NPOESS EDR algorithms. The current version focuses on the Visible/Infrared Imager/Radiometer Suite (VIIRS) subsystem. Future revisions will be extended to the entire NPOESS system.

Furthermore, most of the VIIRS EDR algorithms will require as input one or more types of auxiliary data. In some cases the auxiliary data are obtained from sources that are independent of NPOESS. In other cases recent retrievals from other NPOESS instruments (e.g. Cross-track Infrared Sounder CrIS, and Ozone Mapping and Profiler Suite OMPS) are required and need to be co-located. These data will generally not be reported at the current VIIRS swath locations but rather will be reported at some fixed Earth grid locations or some instrument specific locations in the VIIRS pixel neighborhood.

This document describes the mapping and gridding that will be performed in support of the VIIRS EDR generation algorithms. The approach presented provides a computationally efficient solution that will result in all information needed for the EDR algorithms to match auxiliary data to the VIIRS observations.

1.0 INTRODUCTION

1.1 PURPOSE

This Algorithm Theoretical Basis Document (ATBD) discusses the approaches to re-grid auxiliary data and to grid and re-grid VIIRS Intermediate Products. This document describes the required inputs, practical considerations for post-launch implementation, the assumptions and limitations associated with these approaches, and the description of the re-gridding and gridding techniques.

1.2 SCOPE

This document covers the algorithm theoretical basis for an operational approach to re-gridding and gridding for the production of VIIRS EDRs. There are no gridded VIIRS EDRs in The NPOESS System Specification refers to only one VIIRS gridded product (the deliverable Quarterly Surface Type IP.) Therefore discussion will be limited to the gridding needed to support the generation of VIIRS EDR swath products including the production of gridded IPs. The algorithms discussed herein could be adapted to the production of gridded EDR products, if such a requirement develops at a future date.

This section describes the purpose and scope of this document. Section 2 provides document references. Section 3 provides an overview of the objectives of the re-gridding and gridding, including a review of the requirements, a listing of the products, VIIRS instrument characteristics, and an overview of the major functions of the algorithm (re-gridding, gridding, and compositing). Section 4 contains the algorithm description, including the data processing flow, input data, theoretical description, mathematical description, and practical considerations. Consideration is given to the overall structure, the required inputs, a description of the products, and practical implementation issues. Section 5 contains a listing of references that are cited throughout this document.

1.3 DEFINITIONS

The following definitions are relevant to this ATBD:

Gridding

Gridding is the process of mapping VIIRS swath-based pixel data to grid cells on an Earth model. The VIIRS swath data are collected and processed as a pixelized two-dimensional array. The dimensions are set by the cross-track and along-track directions. We therefore commonly speak of the VIIRS swath data as a two-dimensional set of “pixels”. Each pixel has an Earth location (latitude and longitude) determined by the VIIRS Geolocation algorithm [Y3258]. Gridding, then, consists of determining the value for the VIIRS swath data in the region covered by a VIIRS grid cell.

Compositing

Compositing is the process of combining swath data through data selection, weighting, interpolation, and/or averaging to a single value per grid cell that is representative of the retrieval at that location or area during a specific time period. Compositing will typically involve the combination of data from the current VIIRS swath with previous gridded data according to combination rules that are specific to a given gridded data product.

Auxiliary Data

Those non-VIIRS data required by the EDR algorithms as identified in the EDR Interdependency Report, Document Number D36385 are the auxiliary data.

Re-gridding

Re-gridding is the process of referencing previously gridded VIIRS data or auxiliary data to the VIIRS swath. VIIRS is a cross-track scanner (cf. Section 2.2), Auxiliary data may be representative of locations or areas on a fixed grid or may be representative of points on the surface of the Earth that are not uniformly distributed. Functionally, re-gridding consists of determining the value for the auxiliary or previously gridded VIIRS data in the region covered by the VIIRS pixel.

1.4 REVISIONS

This is the fourth revision of Version 5 of this document, dated 17 September 2004. It contains modifications to make it consistent with the delivered software package.

The third revision of Version 5 of this document was a VIIRS Continuance deliverable dated July, 2004. It contains changes requested by NGST following the delivery of the second revision. The second revision of Version 5 of this document, is a VIIRS Continuance deliverable dated February 11, 2004. It contains changes requested by NGST following the delivery of the first revision. The first revision of Version 5 of this document, is a VIIRS Continuance deliverable dated February 11, 2004. It contains all modifications and additions to the gridding algorithm that have been made under the VIIRS Algorithm Continuance SOW. These include the implementation of nearest neighbor and bilinear interpolation methods

For re-gridding auxiliary data to the VIIRS swath, the implementation of the nearest neighbor method for re-gridding VIIRS gridded data to the VIIRS swath, the implementation of nearest neighbor gridding of VIIRS swath data to a selected VIIRS external grid, defined by a Sinusoidal projection, and the development of compositing methods for ten VIIRS composited IPs stored on the VIIRS grid. The authors wish to thank Drs. Enrique Caponi and Alain Sei for their contributions to this work.

Version 5 was the second working version of this document and is a VIIRS Critical Design Review (CDR) deliverable. It is dated February 2002, and was authored by William P. Byerly, Vincent Grano, Dorlisa Hommel, Ken Jensen, Shawn W. Miller, Richard Sikorski, and Richard Slonaker.

Version 4 was the first version of this ATBD. Its version number was chosen to match the delivery of the previously existing VIIRS EDR ATBDs, which had undergone three previous version releases.

2.0 DOCUMENT REFERENCES

2.1 VIIRS DOCUMENTS

The following VIIRS documents are referenced in this ATBD using their Raytheon SBRS document number in italicized brackets, e.g., *[Y12345]*:

[Y2388]	VIIRS Software Development Plan
[Y2393]	VIIRS Surface Reflectance Unit Level Detailed Design
[Y2398]	VIIRS Surface Albedo ATBD
[Y2400]	VIIRS Vegetation Index (VVI) ATBD
[Y2401]	VIIRS Snow Cover ATBD
[Y2402]	VIIRS Surface Type ATBD
[Y2409]	Sea Ice Age / Edge Motion ATBD
[Y2412]	VIIRS Cloud Mask ATBD
[Y2469]	VIIRS Context Software Architecture
[Y2470]	VIIRS Data Interface Control Document
[Y3258]	VIIRS Geolocation ATBD
[Y3264]	VIIRS Gridding Module Software Architecture

2.2 NON-VIIRS DOCUMENTS

The following non-VIIRS documents are references for this ATBD:

HDF-EOS Library User's Guide for the EMD Project, Volume 1: Overview and Examples, October, 2003, 170-EMD-001.

HDF-EOS Library User's Guide for the EMD Project, Volume 2: Function Reference Guide, October, 2003, 170-EMD-002.

3.0 EXPERIMENT OVERVIEW

3.1 OBJECTIVES OF EARTH GRIDDING

3.1.1 VIIRS EDR Requirements

The objective of Earth gridding is to supply the VIIRS EDR processing algorithms with the input data that is needed to meet the EDR requirements listed in Appendix D of the NPOESS System Specification.

3.1.2 Derived Requirements on VIIRS Gridded IPs

The performance of the VIIRS EDRs depends on the fidelity and efficiency of the re-gridding and gridding algorithms. The EDR quality requirements (accuracy, precision, uncertainty, probability of correct typing) place derived requirements on the quality of the gridded and re-gridded data. Because of the EDR latency requirements, the re-gridding and gridding functions must be capable of co-locating the needed data to the VIIRS pixel locations in a highly efficient way.

3.2 INSTRUMENT CHARACTERISTICS

VIIRS can be pictured as a convergence of three existing sensors, two of which have seen extensive operational use at this writing.

The Operational Linescan System (OLS) is the operational visible/infrared scanner for the Department of Defense (DoD). Its unique strengths are controlled growth in spatial resolution through rotation of the ground instantaneous field of view (GIFOV) and the existence of a low-level light sensor capable of detecting visible radiation at night. OLS has primarily served as a data source for manual analysis of imagery.

The Advanced Very High Resolution Radiometer (AVHRR) is the operational visible/infrared sensor flown on the National Oceanic and Atmospheric Administration (NOAA) Television InfraRed Observation Satellite (TIROS-N) series of platforms (Planet, 1988). Its unique strengths are low operational and production cost and the presence of five spectral channels that can be used in a wide number of combinations to produce operational and research products.

In December 1999, the National Aeronautics and Space Administration (NASA) launched the Earth Observing System (EOS) morning satellite, *Terra*, which includes the Moderate Resolution Imaging Spectroradiometer (MODIS). This sensor possesses an unprecedented array of thirty-two electro-optical to shortwave infrared spectral bands at resolutions ranging from 250 m to 1 km at nadir, allowing for currently unparalleled accuracy in a wide range of satellite-based environmental measurements.

VIIRS will reside on a platform of the National Polar-orbiting Operational Environmental Satellite System (NPOESS) series of satellites. It is intended to be the product of a convergence between DoD, NOAA and NASA in the form of a single visible/infrared sensor capable of satisfying the needs of all three communities, as well as the research community beyond. As such, VIIRS will require three key attributes: high spatial resolution with controlled growth off nadir; minimal production and operational cost; and a sufficient number of spectral bands to satisfy the requirements for generating accurate operational and scientific products.

Figure 1 illustrates the design concept for VIIRS, designed and built by Raytheon Santa Barbara Remote Sensing (SBRS). At its heart is a rotating telescope scanning mechanism that minimizes the effects of solar impingement and scattered light. VIIRS is essentially a combination of Sea-Viewing Wide Field-of-view Sensor (SeaWiFS) fore optics and an all-reflective modification of MODIS/THEMIS aft-optics. Calibration is performed onboard using a solar diffuser for short wavelengths and a blackbody source and deep space view for thermal wavelengths. A solar diffuser stability monitor (SDSM) is also included to track the performance of the solar diffuser. The nominal altitude for NPOESS will be 828 km. The VIIRS scan will therefore extend to about 56 degrees on either side of nadir.

The horizontal spatial resolution (HSR) of bands used to meet threshold Imagery EDR requirements must be no greater than 400 m at nadir and 800 m at the edge of the scan. This led to the development of a unique scanning approach which optimizes both spatial resolution and signal to noise ratio (SNR) across the scan. The concept is summarized in Figure 2 for the imagery bands. The nested lower resolution radiometric bands follow the same paradigm at twice the size.

The VIIRS detectors are rectangular, with the smaller dimension along the scan. At nadir, three detector footprints are aggregated to form a single VIIRS “pixel.” Moving along the scan away from nadir, the detector footprints become larger both along track and along scan, due to geometric effects and the curvature of the Earth. The effects are much larger along scan. At around 32 degrees in scan angle, the aggregation scheme is changed from 3x1 to 2x1. A similar switch from 2x1 to 1x1 aggregation occurs at 45 degrees. The VIIRS scan consequently exhibits a pixel growth factor of only 2 both along track and along scan, compared with a growth factor of 6 along scan which would be realized without the use of the aggregation scheme. Figure 3 illustrates the benefits of the aggregation scheme for spatial resolution. HSI stands for horizontal sampling interval, the distance between centers of aggregated pixels along-scan. GSD is the ground sample distance between individual detector footprints.

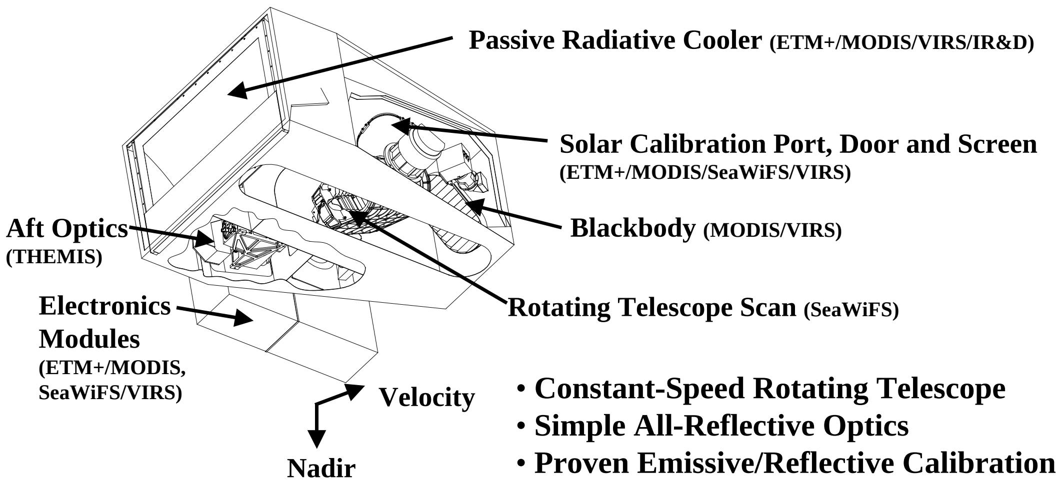

Figure 1. Summary of VIIRS design concepts and heritage.

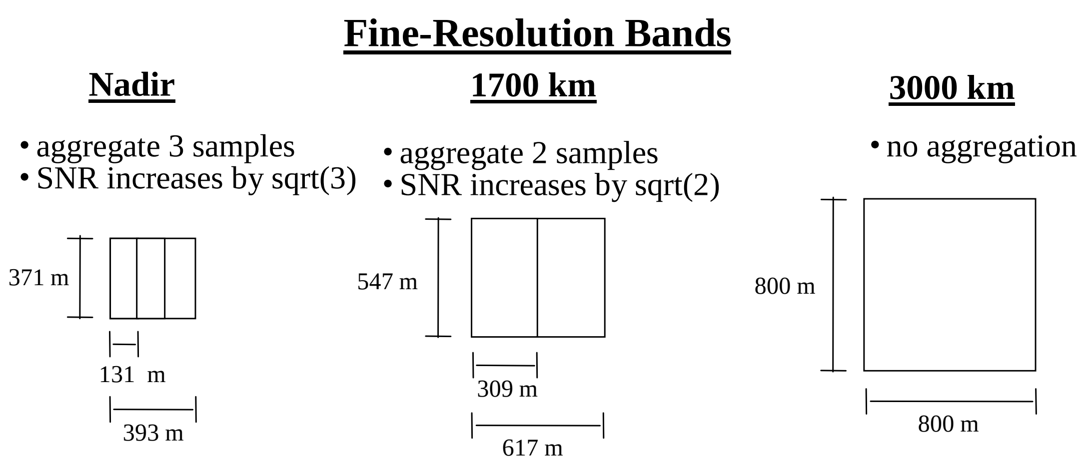

Figure 2. VIIRS detector footprint aggregation scheme for building "pixels."

The sizes in Figure 2 are approximate. Please refer to the VIIRS Sensor Specification for up-to-date values.

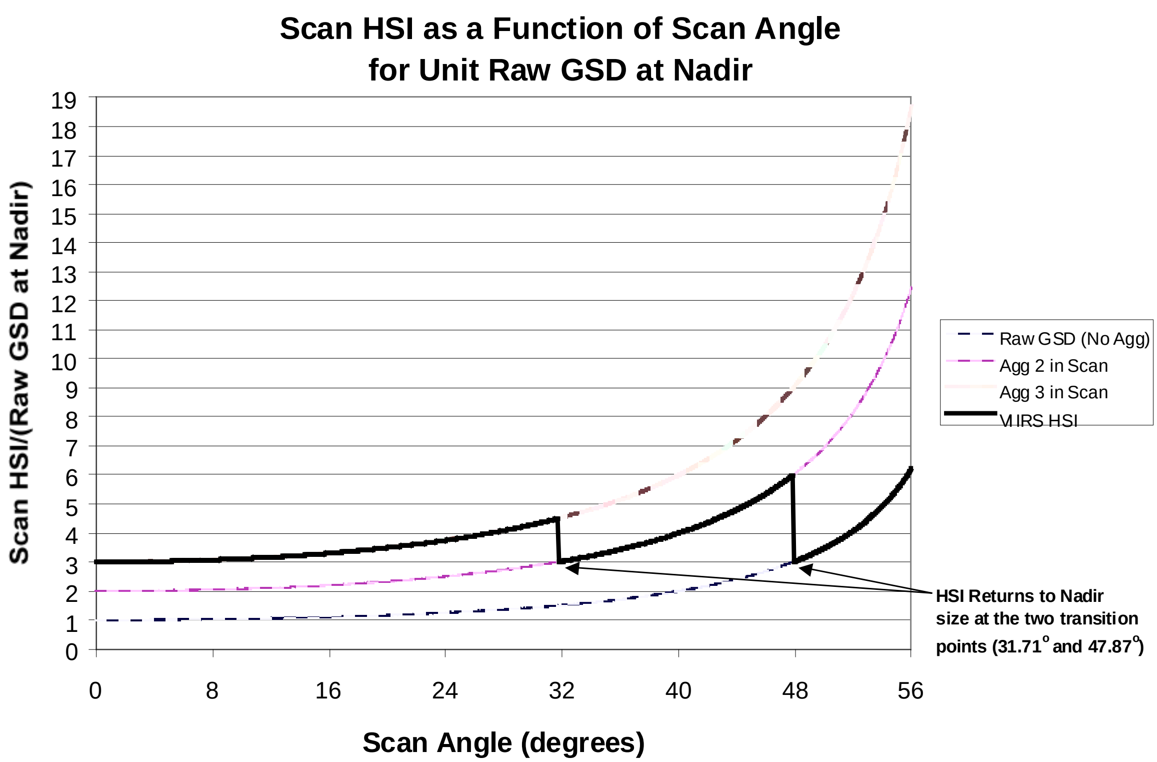

Figure 3. Benefits of VIIRS aggregation scheme in reducing pixel growth at edge of scan.

Switch-point angles in Figure 3 are approximate. Please refer to the VIIRS Sensor Specification for up-to-date values. This scanning approach is extremely beneficial for the retrieval of land products such as the NDVI.

The VIIRS gridded reflectance IPs (c.f. Sections 4.3.4.1, 4.3.4.2, and 4.3.4.3) consist of nine VIIRS spectral bands. The positioning of the bands is summarized in Table 1.

Table 1. VIIRS spectral bands used in Gridded Products

Band Name[a]	Center (microns)	Width[b] (microns)
M1	.412	.020
M2	.445	.020
M3	.488	.020
M4	.555	.020
M5	.672	.020
M7	.865	.039
M8	1.24	.020
M10	1.61	.060
M11	2.25	.050

[a] M indicates band with a NADIR resolution of 750 m. [b] full width half maximum (FWHM)

3.3 EARTH GRIDDING STRATEGY

Earth gridding includes two distinct functions, re-gridding and gridding.

Re-gridding is a process of referencing auxiliary data and previously gridded IPs to the VIIRS pixel locations. The purpose is to provide an auxiliary data set in the same two-dimensional array form as the VIIRS swath data, so that the EDR processing algorithms can match the auxiliary data to the VIIRS data. Auxiliary data may be representative of locations or areas on a fixed grid or may be representative of points on the surface of the Earth that are not uniformly distributed. The spatial resolution of the auxiliary data sources (cf. Table 2) ranges from less than 1 km to greater than 100 km, so is generally coarser than the spacing between the centers of VIIRS pixels. Re-gridding requires geolocation of the pixels in the VIIRS swath. The re-gridding products are required inputs to the EDR processing algorithms. Re-gridding is therefore an activity that occurs between SDR processing (geolocation) and EDR processing.

Gridding is the process of accumulating VIIRS pixel data into grid cells on an Earth model. Most gridded products are composites of many observations obtained at the same location over a specified time interval. The compositing process combines these data through data selection, weighting, interpolation, and/or averaging to a single value per grid cell that is representative of the retrieval at that location or area during a specific time period. The combination rules are specific to each gridded product (cf. Section 4.3.4). Gridding generally requires processed data for the current VIIRS swath. It is therefore an activity that occurs after the EDR production process.

4.0 ALGORITHM DESCRIPTION

4.1 PROCESSING OUTLINE

The Gridding module contains many software units that re-grid, grid, and composite a variety of input data. The process flow is therefore complex. Detailed process flow architecture can be found in the Gridding Module Level Software Architecture document *[Y-3264].* A high-level process flow is illustrated in Figure 4.

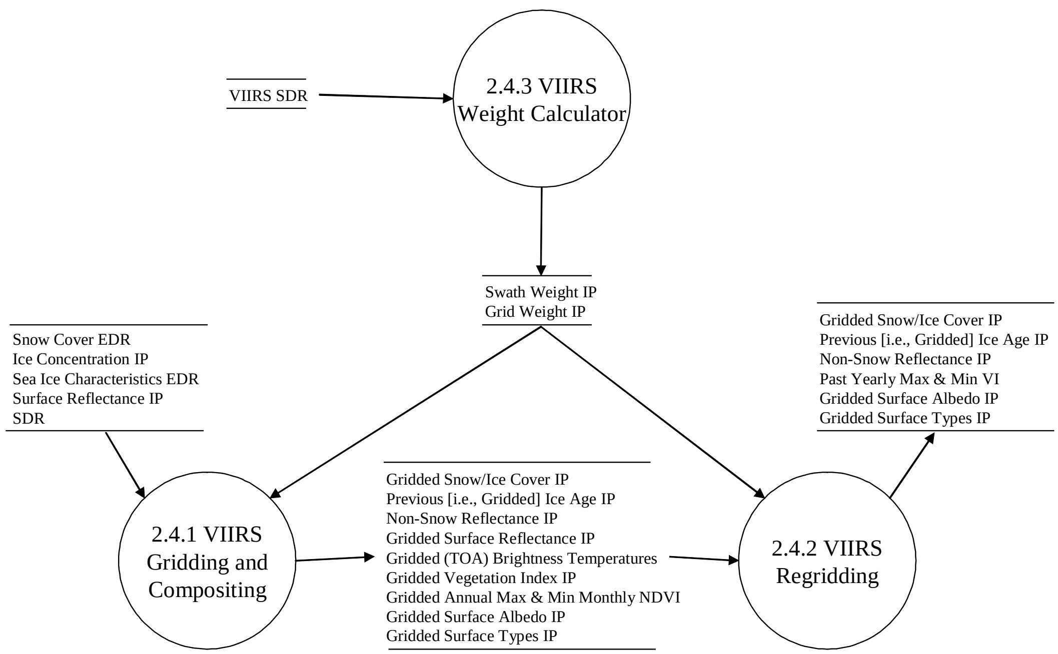

Figure 4. Gridding / Re-gridding Module Level 3 Software Architecture

Re-gridding and gridding will be performed at various times relative to the operational processing. Some gridding will be performed during the processing of mission data, and some will be performed during post-EDR processing.

In general, the re-gridding of auxiliary data and required gridded IPs will be performed during the processing of mission data, as soon as the imagery and moderate resolution, height-adjusted geolocation IPs are ready. Auxiliary data will be interpolated to pixel locations and previously gridded IPs will be either area weighted or their values will be determined by nearest neighbor assignment, depending on the IP.

The DEM will be processed in the main production processing of the VIIRS SDR as part of geolocation. The DEM processing will yield geoid and terrain height. It does not map the DEM to swath level. A land-water-coastline indicator will be derived from the auxiliary land-water mask as part of the generation of the Cloud Mask IP. Each of these will be determined at the VIIRS pixel locations and stored in each SDR file.

Re-gridding will provide the information needed for EDR algorithms to efficiently access auxiliary data that is co-located with VIIRS pixels. Re-gridding will not perform any selection or interpolation among Auxiliary data that may be available for different times.

It is expected that gridding of most VIIRS products will be a post-processing activity, so as not to interfere with operational EDR production. In each case, these gridded VIIRS data will be available for EDR processing of subsequent swaths.

4.2 ALGORITHM INPUT

4.2.1 VIIRS Data

The following VIIRS swath data will be input to the VIIRS gridding algorithms:

- SDR
- Ice Concentration IP
- Sea Ice Characterization EDR
- Surface Reflectance IP
- Snow Cover EDR

The following VIIRS gridded data will be input to the VIIRS gridding algorithms:

- Gridded Daily Surface Reflectance IP
- Gridded Monthly Surface Reflectance IP
- Gridded Monthly Brightness Temperature IP
- Gridded Monthly Vegetation Index IP
- Gridded BRDF Archetypal IP

The following VIIRS data will be computed on the Earth grid from already gridded IPs:

- Gridded Surface Albedo IP
- Gridded Quarterly Surface Types IP
- Gridded Annual Max/Min Normalized Difference Vegetation Index (NDVI) IP
- Gridded Biomes IP

The following Earth gridded VIIRS data will be re-gridded for every VIIRS granule:

- Gridded Surface Albedo IP (MOD resolution; required by Surface Albedo and Cloud Optical Properties)
- Gridded Quarterly Surface Types IP (MOD resolution; required by Aerosol Optical Thickness, Cloud Optical Properties, Snow Cover, and Surface Types)
- Gridded Quarterly Surface Types IP (IMG resolution; required by Vegetation Index)
- Gridded Annual Max/Min Monthly NDVI IP (MOD resolution; required by Surface Types EDR)
- Gridded Previous Ice Age IP (IMG resolution; required by Sea Ice)
- Gridded Non-snow Surface Reflectance IP (MOD resolution; required by Snow Cover)
- Gridded Snow/Ice Cover IP (MOD resolution; required by Cloud Mask)

4.2.2 Non-VIIRS Data

Auxiliary data from a variety of sources and in a variety of formats will be re-gridded. These auxiliary data are identified in the VIIRS Data Interface Control Document *[Y2470]*. Table 2 summarizes the sources and types of auxiliary data.

Table 2. Auxiliary Data

Data Set	Source	File Format	Reference	Freq
Aerosol Climatology	GACP/GEWEX	ASCII (1° grid)	http://gacp.giss.nasa.go v/retrievals/	Static
Global Land Classification	USGS	Flat Binary	http://edcdaac.usgs.gov /glcc/globdoc2_0.html	Static
Digital Bathymetry Data	NOAA ETOPO-2	Flat Binary	http://www.ngdc.noaa.g	Static

			ov/mgg/fliers/01mgg04.html	
Nitrate Depletion Temperatures	Kendall Carder	HDF	Equal angle raster 1024 x 2048	Static
Total Column Ozone	NCEP GDAS	GRIB	http://www.nws.noaa.gov/climate.html	6 hours
Surface Pressure	NCEP GDAS	GRIB	http://www.nws.noaa.gov/climate.html	6 hours
U & V wind components	NCEP GDAS	GRIB	http://www.nws.noaa.gov/climate.html	6 hours
Temperature Profile	NCEP GDAS	GRIB	http://www.nws.noaa.gov/climate.html	6 hours
Surface Air Temperature	NCEP GDAS	GRIB	http://www.nws.noaa.gov/climate.html	6 hours
Precipitable Water	NCEP GDAS	GRIB	http://www.nws.noaa.gov/climate.html	6 hours
Surface Relative Humidity	NCEP GDAS	GRIB	http://www.nws.noaa.gov/climate.html	6 hours
Relative Humidity Profile	NCEP GDAS	GRIB	http://www.nws.noaa.gov/climate.html	6 hours
Geopotential Height Profile	NCEP GDAS	GRIB	http://www.nws.noaa.gov/climate.html	6 hours
MSL Pressure	NCEP GDAS	GRIB	http://www.nws.noaa.gov/climate.html	6 hours
Tropopause Height	NCEP GDAS	GRIB	http://www.nws.noaa.gov/climate.html	6 hours
Global Snow/Ice Cover (Northern Hemisphere)	NOAA OSPO (OSDPD)	Flat Binary	http://satepsanone.nesdis.noaa.gov/northern_hemisphere_multisensor.html	Daily
Global Snow/Ice Cover (Southern Hemisphere)	NOAA OSPO (OSDPD)	Flat Binary	http://satepsanone.nesdis.noaa.gov/southern_hemisphere_multisensor.html	Daily

4.3 THEORETICAL DESCRIPTION OF EARTH GRIDDING

4.3.1 The VIIRS Grid

The Sinusoidal Projection implemented in the HDF-EOS Library for the Earth Observing System Data and Information System (EOSDIS) Core System (ECS) Project has been used as a template the VIIRS global grid. The VIIRS global grid is based the Sinusoidal Projection. This approach uses the United States Geological Survey (USGS) General Cartographic Transformation Package (GCTP) to define, create, and make use of gridding functions.

4.3.1.1 Considerations

VIIRS pixel size – select a grid size that is close to the spacing between the moderate resolution band pixels. The latitudinal grid size will be approximately 926 m.

Number of cells – select a grid size that will result in a reasonable number of grid cells, considering storage and processing efficiency, and convenient aggregation of cells.

Layout of cells – maintain a simple relationship between latitude and longitude and grid boundaries. Avoid grid cells that straddle the Equator or a Pole due to physical and mathematical considerations.

4.3.1.2 Grid Definition

The VIIRS grid will be defined and created using GCTP. The grid parameters are adapted from those used by the MODIS project. MODIS' projection parameters can be found at http://modland.nascom.nasa.gov/developers/is_tiles/is_gctp.html. Table 3 contains the projection parameters for VIIRS.

Table 3. Sinuzoidal Grid parameters for the USGS General Cartographic Transformation Package (GCTP).

Num	Parameter	Value	Description
0	Sphere	6371007.181	Radius of reference (meters) sphere
1-3		0.0	not used
4	CentMer	0.0	Longitude of the central meridian
5		0.0	not used
6	FE	0.0	False Easting in the same units as the sphere radius
7	FN	0.0	False Northing in the same units as the sphere radius
8	NZone	21600.0	Number of equally spaced latitudinal zones (rows). Must be 2 or larger and even.
9		0.0	not used
10	RFlag	0.0	Right justify columns flag is used to indicate what to do with zones with an odd number of columns. If it has a value of 0 or 1 it indicates the extra column is on the right (zero) or left (one) of the projection y-axis. If the flag is set to 2 the number of columns are calculated so there are always an even number of column in each zone.
11-14		0.0	not used

4.3.2 Grid Cell Identification

The VIIRS grid will be defined and created using GCTP, as described in Section 4.3.1. GCTP provides the mapping from latitude / longitude coordinates to X / Y coordinates. Conversion factors are then applied to map X / Y coordinates to grid cell coordinates.

4.3.3 Gridding/Re-gridding Methods

Each of the methods discussed below can be performed in the native space of its source grid, or its target grid. In general, these algorithms are easier to implement in geographic (lat/lon) space. Therefore, the current design will perform all interpolations in geographic space.

4.3.3.1 Nearest Neighbor

The nearest neighbor interpolation method (Bracewell, 1995) assumes a 2-dimensional set of data points (x_N,y_N) is available. The interpolation is generated on a rectangular grid, where the value of each interpolated point, (x_{NN},y_{NN}) is set to the value of the nearest of the four points surrounding the original indexed point on the grid (cf. Figure 5).

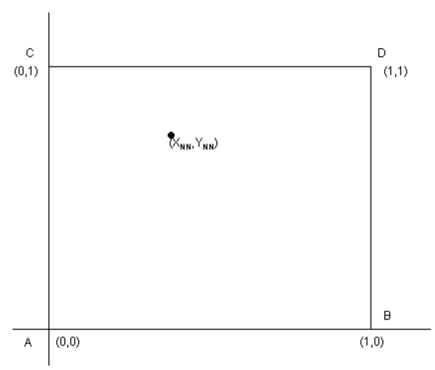

Figure 5. Nearest Neighbor mapping. The resampled pixels are mapped to the nearest of data points (0,0), (0,1), (1,0) and (1,1).

The nearest neighbor technique described may be implemented using logical comparisons instead of multiplications, therefore it runs faster than other interpolation techniques. By comparison, with other techniques, it introduces some high-frequency noise, which may degrade the quality of the resultant image.

4.3.3.2 Bilinear Interpolation

The bilinear interpolation method: (http://www.wisdom.weizmann.ac.il/~maksimf/ex5/Resample.html) assumes a 2-dimensional set of data points (x_N,y_N) is available. The interpolation is generated on a rectangular grid (see Figure 6).

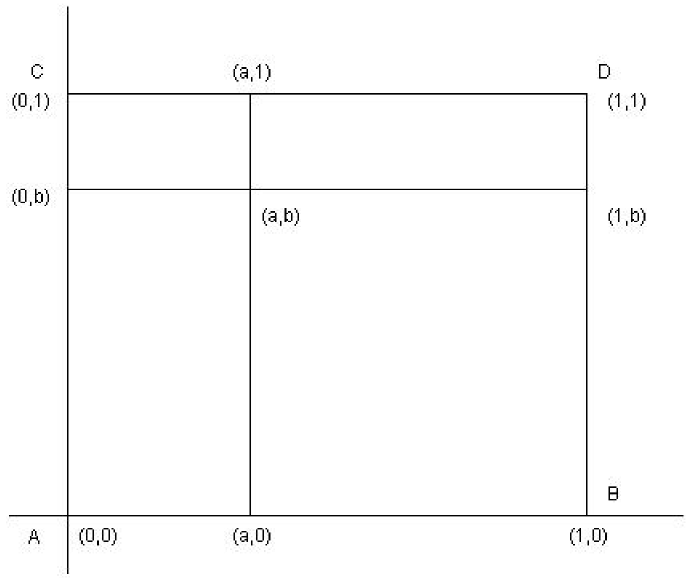

Figure 6. Bilinear interpolation. The resampled pixels are mapped to data points (0,0), (0,1), (1,0) and (1,1).

Let the resampled pixel from the set (x_N,y_N) be called $F_{a,b}$, i.e. each pixel at location (x,y) is $F_{x,y}$.

It is necessary to obtain the data value at each resampled pixel.

This can be achieved in two stages:

First define $F_{a,0} = (1\text{-}a)\ F_{0,0} + a\ F_{1,0}$, and $F_{a,1} = (1\text{-}a)\ F_{0,1} + a\ F_{1,1}$.

Then $F_{a,b} = (1\text{-}b)\ F_{a,0} + b\ F_{a,1} = (1\text{-}b)(1\text{-}a)\ F_{0,0} + (1\text{-}b)\ a\ F_{1,0}. + b(1\text{-}a)\ F_{0,1} + b\ a\ F_{1,1}$.

If any of the existing values ($F_{a,b}$) contain fill values, their weights are set to zero and the weights are re-normalized. If all four ($F_{a,b}$) contain fill values, the interpolated value will be set to its fill value.

4.3.3.3 Cubic Convolution

Cubic convolution shall not be implemented in any portion of the Gridding/Re-gridding Component. The following description remains for historical reasons.

Traditional piecewise cubic convolution, PCC, (Reichenbach and Geng, 2003) has been in use since the 1970's. The 1-D PCC kernel is defined as a separable generalization of a symmetric generalization of a one-dimensional function consisting of cubic polynomial pieces between knots {-2, -1, 0, 1, 2}. PCC imposes constraints to insure continuity and smoothness leaving one parameter that can be used to tune the kernel.

Pixel samples from a digital image p are convolved with a piecewise –cubic kernel f, giving the continuous result r.

$$r(x) = p[m]f(\ -m) \text{ for } -\infty < x < \infty. \qquad (1)$$

A symmetric kernel is defined piecewise by cubic polynomials in the intervals:

$|x| \le 1$ and $1 < |x| \le 2$. For $|x| > 2$, the kernel is zero.

The general form is given by:

$$f(x) = \begin{cases} a_3\,|x|^3 + a_2\,|x|^2 + a_1\,|x| + a & \text{if } |x| \le 1 \\ b_3\,|x|^3 + b_2\,|x|^2 + b_1\,|x| + b_0 & \text{if } 1 < |x| \le 2 \\ 0 & \text{otherwise.} \end{cases} \qquad (2)$$

The seven constraints, not shown here, leave one degree of freedom, identified with the slope of the kernel at x=1. Interpolation requires f(0)=1.

For the 2-D case, the general piecewise, symmetric polynomial with degree six on the interval [-2,2] x [-2,2] is defined by the function,

$$f(x,y) = \begin{cases} f_a(x,y) = \sum_{j=0}^{6} \sum_{k=0}^{6-j} a_{jk} x^j y^k & 0 \le x \le 1,\ 0 \le y \le 1 \\ f_b(x,y) = \sum_{j=0}^{6} \sum_{k=0}^{6-j} b_{jk} x^j y^k & 0 \le x \le 2,\ 0 \le y \le 1 \\ f_c(x,y) = \sum_{j=0}^{6} \sum_{k=0}^{6-j} c_{jk} x^j y^k & 0 \le x \le 2,\ 1 \le y \le 2 \\ f_d(x,y) = \sum_{j=0}^{6} \sum_{k=0}^{6-j} d_{jk} x^j y^k & 0 \le x \le 1,\ 1 \le y \le 2 \end{cases} \qquad (3)$$

The constraints, again not shown here for simplicity, are for continuity between pieces, for a continuous first derivative between pieces and for a flat-field response and interpolation. In combination they reduce the number of free parameters from 112 to 2.

With the constraints, the 2-D PCC kernel can be written as the sum of the traditional, separable kernel f_s and an additional term weighted by an optimizing parameter, β,

$$f(x,y) = f_s(x,y) + \beta\, f_n(x,y) \qquad (4)$$

where $f_n(x,y) = f_1(x)\, f_1(y)$ (5)

An expansion of (4) gives

$$f(x,y) = (f_0\,(x) + \alpha\, f_1(x))\,(f_0\,(y) + \alpha\, f_1(y)) \;+ \beta\, f_n\,(x) f_1(y) \qquad (6)$$

Where α is the first derivative, and

$$f_0(x) = \begin{cases} |x|^3 - 3|x|^2 + 1 & \text{if } |x| \le 1 \\ 0 & \text{otherwise.} \end{cases} \qquad (7)$$

$$f_1(x) = \begin{cases} |x|^3 - |x|^2 & \text{if } |x| \le 1 \\ |x| - 5|x|^2 + 8|x| - 1 & \text{if } 1 \le |x| \le 2 \\ 0 \quad \text{otherwise.} \end{cases} \qquad (8)$$

For optimal results for the separable case, α = -1, and β =0. For the non-separable case, β can be expressed as a function of the scene power spectrum and the kernel components with parameter α, not shown here.

4.3.3.4 Area Weighting

The area weighting method used for both gridding and re-gridding on VIIRS leverages MODIS heritage (Yang and Wolfe). It uses a technique called “cake-cutting” to determine the intersections of the footprints of overlapping pixels and grid cells. From this information, a weight proportional to the area of the overlap can be assigned to the pixel/cell pair. The following subsections discuss how these weights are used for gridding and re-gridding, some computational considerations, and the concept of volume weighting.

4.3.3.4.1 Gridding

In the gridding case, these weights are calculated with respect to the grid cell. These “forward” weights can then be used to calculate an area-weighted average for a particular satellite pass, as shown in Eq (9).

$$C_j = \Sigma P_i W_{i,j} \qquad (9)$$

Where C_j represents the area weighted value at cell j, P_i is the data value at an overlapping pixel, and $W_{i,j}$ is the weight associated with the pixel/cell pairing.

Subsequent passes of the satellite will have the same area weighting technique applied to produce coincident area weighted results. The data from all passes within the aggregation period are combined using the compositing method prescribed for each product.

4.3.3.4.2 Re-Gridding

In the re-gridding case, the weights are calculated with respect to the pixel. These "reverse" weights can be used to resample gridded data back into VIIRS swaths, as shown in Eq (10).

$$P_i = \sum C_j W_{j,i} \qquad (10)$$

Where P_i represents the area weighted value at pixel i, C_j is the data value at an overlapping cell, and $W_{j,i}$ is the weight associated with the cell/pixel pairing.

4.3.3.4.3 Computational Considerations

Although the weights used for gridding and re-gridding are different, the information and calculations required to produce the weights are largely the same. Therefore, it is computationally convenient to produce weights for gridding and re-gridding at the same time. The re-gridding weights are used immediately to accomplish any re-gridding required for EDR processing. The gridding weights are saved until such time as the output products are available for gridding.

4.3.3.4.4 Volume Weighting

In addition to accounting for the overlapping areas of the pixels and grid cells, it is also necessary to account for the temporal shape (or integration envelope) of the detector footprint that gives rise to the pixel value. This envelope can be thought of as comprising a third dimension of each pixel. With this additional information, a more accurate estimate of a pixel's contribution to a grid cell can be made.

Recall that there are three aggregation zones across the VIIRS scan (c.f. Section 3.2). This means that there are three distinct integration envelopes that must be accommodated. For VIIRS, then, the integration envelope is modeled by adding together the roughly triangular envelope shapes of each detector used in the aggregation zone. Figure 7 shows the result of this operation.

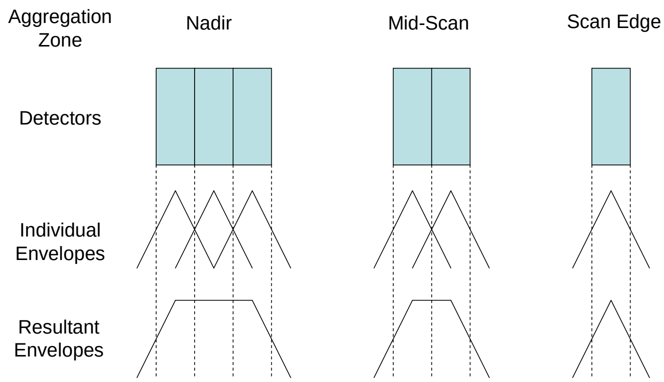

Figure 7. Integration envelopes of the VIIRS aggregation zones.

Although the above discussion refers only to gridding, similar considerations applied to the calculation of the “reverse” weights will result in volume weighted re-gridding.

4.3.4 Generation of Gridded VIIRS IPs

The gridded products will be files that are created and maintained by GCTP capabilities and the HDF-EOS Grid API.

For those gridded products that are averages over some time period (daily, bi-weekly or 17 day, monthly, or quarterly) a new file is created at the beginning of the time period, then added to as the time period continues. At the end of the specified time period the gridded product will be complete.

Details regarding the definition and the rules for data selection, interpolation, and/or averaging vary for each gridded product.

4.3.4.1 Gridded Daily Surface Reflectance IP

The Gridded Daily Surface Reflectance (GDSR) IP is required for producing the Gridded Surface Albedo IP. Table 4 gives the output data array and structure.

Table 4. Gridded Daily Surface Reflectance (GDSR) IP array structure.

Dimension	Elements
Observations	up to 15 observation passes per day
Global Grid (Spatial)	Grid Cell Row and Column Numbers
Bands	M1,M2,M3,M4,M5,M7,M8,M10, M11
Parameter	Reflectance(Bands, Observations, Grid), SolarZenith(Bands, Observations, Grid),

	View Zenith(Bands, Observations, Grid), RelativeAzimuth(Bands, Observations, Grid),

The GDSR algorithm requires that reflectance observations from different satellite passes must be stored. Within a pass, a compositing process is applied to aggregate multiple observations in one grid cell. The aggregation algorithm discards all oceanic and night-time pixels. The greatest weight neighbor from the remaining pixels is chosen to represent the output grid cell provided the quality fields of this greatest weight neighbor satisfies all of the following conditions:

- Cloud mask = not confidently cloudy
- Thin cirrus = no thin cirrus

When the grid for the current day has been completed, a new GDSR file will be created to continue with the following day's observations. At the time of its use, the GDSR IP will consist of data from the sixteen days prior to the current day, plus a partially completed grid for the current day. The use of the sixteen-day Daily Gridded Surface Reflectance IP for the Gridded Surface Albedo IP is a heritage from MODIS Albedo algorithm [Schaaf et al., 2002; Strahler *and* Muller 1996].

4.3.4.2 Gridded Monthly Surface Reflectance IP

The Gridded Monthly Surface Reflectance (GMSR) IP, together with the Gridded Monthly Vegetation Index (GMVI) IP and Gridded Monthly Brightness Temperature (GMBT) IP to be discussed in the following sections, is required by the Quarterly Surface Type (QST) IP Unit to produce three Gridded IPs: the Gridded Quarterly Surface Type (GQST) IP, Gridded Biomes IP, and Gridded Annual Maximum and Minimum Monthly NDVI (GAMMMN) IP. For further details on the Surface Type algorithm, the reader is directed to the VIIRS Surface Type ATBD *[Y2402]*.

The GMSR IP is one of three monthly IPs. The monthly IPs, i.e., the GMSR IP, the GMVI IP (c.f. Section 4.3.4.4), and the GMBT IP (c.f. Section 4.3.4.5), also called monthly composites, are generated using the compositing procedure described in section 4.3.7. Table 5 shows the structure of this IP and the VIIRS bands contained in it.

Table 5. Gridded Monthly Surface Reflectance (GMSR) IP array structure.

Dimension	Elements
Global Grid (Spatial)	Grid Cell Row and Column Numbers
Parameter	Monthly composited values for VIIRS Bands M1, M2, M3, M4, M5, M7, M8, M10, and M11

4.3.4.3 Monthly Non-snow Surface Reflectance IP

The Monthly Non-snow Surface Reflectance IP (MNSR) is used by the Snow Cover EDR, which characterizes the non-snow background in a given pixel to estimate the snow fraction using spectral mixture analysis. For further details on the snow fraction algorithm, the reader is directed to the VIIRS Snow Cover ATBD *[Y2401]*.

The structure of the MNSR IP is shown in Table 6.

Table 6. Monthly Non-snow Surface Reflectance (MNSR) IP array structure.

Dimension	Elements
Global Grid (Spatial)	Grid Cell Row and Column Numbers
Parameter	Composited Reflectance in VIIRS Bands M1, M2, M3, M4, M5, M7, M8, M10, M11

The MNSR IP is a running, monthly composite of surface reflectance. It is identical to the GMSR IP, except that pixels containing snow are explicitly rejected in the compositing algorithm. During a month, the non-snow surface reflectance corresponding to the CV-MVC “best estimate” of (the non-snow) VI is kept in a running fashion. At the end of a month, the MNSR IP contains the final result, which can then be nadir adjusted via the BRDF method, using coincident BRDF information from the Gridded Surface Albedo IP. The MNSR is used by the Snow/Ice Cover EDR algorithm.

4.3.4.4 Gridded Monthly Vegetation Index IP

As mentioned in the previous section, the Gridded Monthly Vegetation Index (GMVI) IP is required for use by the Quarterly Surface Type IP Unit to produce the GQST IP, the Gridded Biomes IP, and the GAMMMN IP. For further details on the Surface Type algorithm, the reader is directed to the VIIRS Surface Type ATBD *[Y2402]*.

The structure of the GMVI IP is shown in Table 7. It is generated using the compositing procedure described in section 4.3.7 , and contains the TOC NDVI value for each month. The NDVI value in this IP is calculated using the following equation:

$$NDVI = (M7 - M5)/(M7 + M5) \qquad (11)$$

If the CV-MVC compositing method is used, M5 and M7 are the surface reflectance values from the “best” directional VIIRS observation of a month selected according to the compositing criteria. Otherwise if the BRDF based compositing method is used, M5 and M7 are derived nadir measurements based on BRDF models fitted to qualified directional VIIRS observations. Both the CV-MVC and BRDF based compositing methods are described in section 4.3.7. The physics behind the NDVI are described in the VIIRS Vegetation Index (VVI) ATBD *[Y2400]*.

Table 7. Gridded Monthly Vegetation Index (GMVI) IP array structure.

Dimension	Elements
Global Grid (Spatial)	Grid Cell Row and Column Numbers
Parameter	Composited Normalized Difference Vegetation Index (NDVI)

4.3.4.5 Gridded Monthly Brightness Temperature IP

The Gridded Monthly Brightness Temperature (GMBT) IP is used by the Quarterly Surface Type IP Unit. For further details on the Surface Type algorithm, the reader is directed to the VIIRS Surface Type ATBD *[Y2402]*.

The structure of the GMBT IP is shown in Table 8.

. It contains one top-of-atmosphere brightness temperature value per month for each of the VIIRS moderate resolution thermal bands listed in Table 8.

. For each band, the composited value is selected using the CV-MVC compositing method, i.e., the value is the “best” directional VIIRS observation of a month selected according to the compositing criteria. The BRDF based compositing method does not apply to the thermal bands. The CV-MVC compositing method is described in section 4.3.7.

Table 8. Gridded Monthly Brightness Temperature (GMBT) IP array structure.

Dimension	Elements
Global Grid (Spatial)	Grid Cell Row and Column Numbers
Parameter	Composited Brightness Temperature in VIIRS Bands M12, M13, M14, M15, and M16

4.3.4.6 Gridded Quarterly Surface Types IP

The operational Surface Type EDR, reported on each VIIRS swath, will be produced from the global 1 km VIIRS Gridded Quarterly Surface Types (GQST) IP. The GQST IP is produced once every three months. Both the GQST IP (on the global grid) and the instantaneous EDR (on the swath) will include all 17 IGBP classes.

The VIIRS Quarterly Surface Type IP algorithm will be run in a supervised classification mode, using global training data specifically tailored to the 17 IGBP surface types (see Table 9), and temporal metrics developed from 12 consecutive months of VIIRS moderate resolution data called monthly composites, or monthly IPs. These monthly IPs, the GMSR IP, GMVI IP and GMBT IP, have been described in previous sections. Other inputs to the VIIRS Quarterly Surface Type IP algorithm include a global 1 km digital elevation model (DEM) and a gridded raster file depicting the distribution of urban areas based on the Digital Chart of the World. Both inputs have been mapped into the VIIRS grid using external reprojection tools implemented in commercial image processing packages.

Table 9. IGBP surface type definitions (from Strahler et al., 1996a).

IGBP Surface Type Number and Name	Definition
1) Evergreen Needleleaf Forests	Lands dominated by woody vegetation with a percent cover >60% and height exceeding 2 meters. Almost all trees remain green all year. Canopy is never without green foliage.
2) Evergreen Broadleaf Forests	Lands dominated by woody vegetation with a percent cover >60% and height exceeding 2 meters. Almost all trees and shrubs remain green year round. Canopy is never without green foliage.
3) Deciduous Needleleaf Forests	Lands dominated by woody vegetation with a percent cover >60% and height exceeding 2 meters. Consists of seasonal needleleaf tree communities with an annual cycle of leaf-on and leaf-off periods.
4) Deciduous Broadleaf Forests	Lands dominated by woody vegetation with a percent cover >60% and height exceeding 2 meters. Consists of broadleaf tree communities with an annual cycle of leaf-on and leaf-off periods.
5) Mixed Forests	Lands dominated by trees with a percent cover >60% and height exceeding 2 meters. Consists of tree communities with interspersed mixtures or mosaics of the other four forest types. None of the forest types exceeds 60% of landscape.
6) Closed Shrublands	Lands with woody vegetation less than 2 meters tall and with shrub canopy cover >60%. The shrub foliage can be either evergreen or deciduous.
7) Open Shrublands	Lands with woody vegetation less than 2 meters tall and with shrub canopy cover between 10-60%. The shrub foliage can be either evergreen or deciduous.
8) Woody Savannas	Lands with herbaceous and other understory systems, and with forest canopy cover between 30-60%. The forest cover height exceeds 2 meters.
9) Savannas	Lands with herbaceous and other understory systems, and with forest canopy cover between 10-30%. The forest cover height exceeds 2 meters..
10) Grasslands	Lands with herbaceous types of cover. Tree and shrub cover is less than 10%.
11) Permanent Wetlands	Lands with a permanent mixture of water and herbaceous or woody vegetation. The vegetation can be present in either salt, brackish, or fresh water.
12) Croplands	Lands covered with temporary crops followed by harvest and a bare soil period (*e.g.*, single and multiple cropping systems). Note that perennial woody crops will be classified as the appropriate forest or shrub land cover type.
13) Urban and Built-Up Lands	Lands covered by buildings and other man-made structures.
14) Cropland/Natural Vegetation Mosaics	Lands with a mosaic of croplands, forests, shrubland, and grasslands in which no one component comprises more than 60% of the landscape.
15) Snow and Ice	Lands under snow/ice cover throughout the year.
16) Barren	Lands with exposed soil, sand, rocks, or snow and never has more than 10% vegetated cover during any time of the year.
0) Water Bodies	Oceans, seas, lakes, reservoirs, and rivers. Can be either fresh or salt-water bodies.

Figure 8 shows the process flow for the VIIRS Gridded Quarterly Surface Types IP.

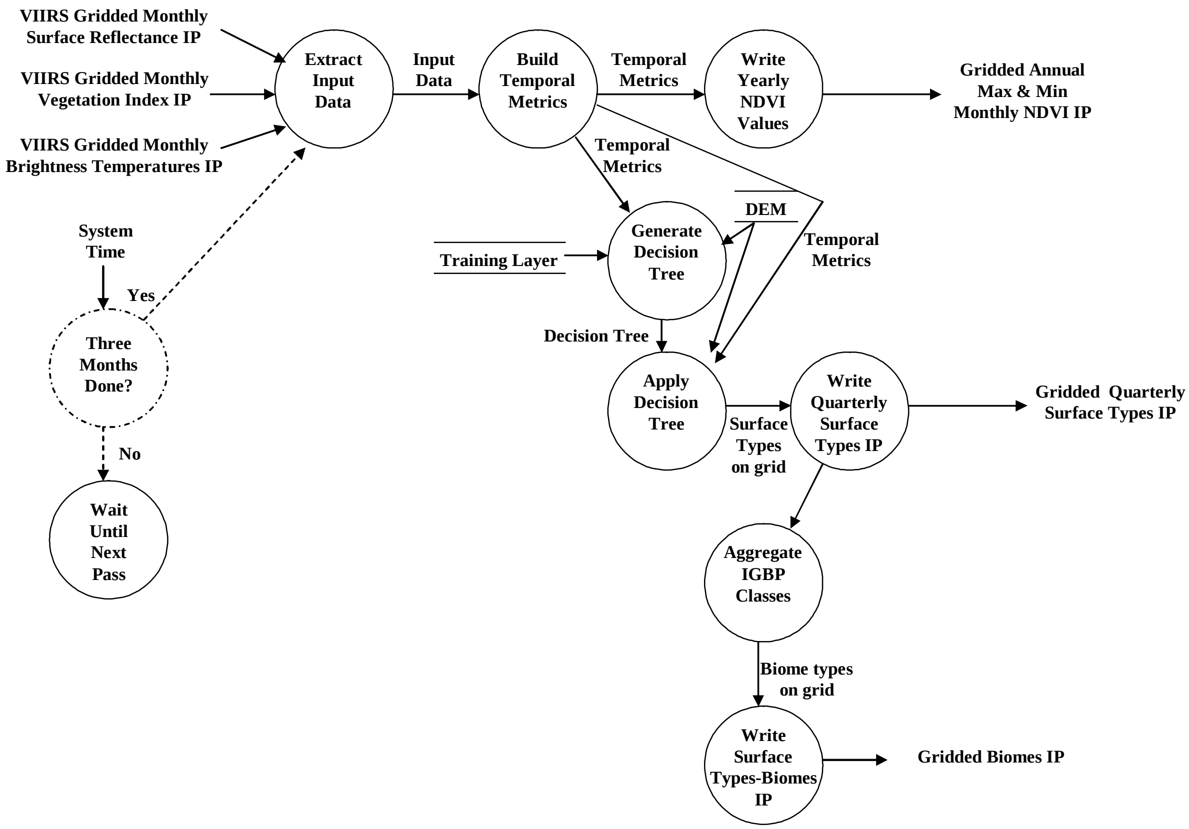

Figure 8. Process flow for the VIIRS Quarterly Surface Types IP.

Table 10 lists the input data to the unit that produces the VIIRS Quarterly Surface Types IP.

Table 10. Indexing of inputs for Quarterly Surface Types IP

Name	Type	Description
VIIRS Gridded Monthly Surface Reflectance IP	Input	VIIRS Gridded Monthly Surface Reflectance IP for the past year
VIIRS Gridded Monthly Vegetation Index IP	Input	VIIRS Gridded Monthly Vegetation Index IP for the past year
VIIRS Gridded Monthly Brightness Temperatures IP	Input	VIIRS Gridded Monthly Brightness Temperatures IP for the past year
GTOPO30	Input	Global 30 Arc-Second Digital Elevation Data Set
DCW/Urban	Input	Urban delineated in the Digital Chart of the World
Training Layers	Input	Predefined areas of the 17 IGBP surface types obtained the updated 1km global training areas

A supervised decision tree program, C5.0, is used to generate the GQST IP. A detailed description of the algorithm of a previous version of this program, C4.5, is provided by Quinlan (1993). The reader is referred to Section 3.4 of the VIIRS Surface Type ATBD *[Y2402]* for details on the classifier, the surface typing algorithm and the generation of the Gridded Quarterly Surface Types IP.

4.3.4.7 Quarterly Continuous Fields IP

The Gridded Quarterly Surface Type (GQST) IP is one of the three IPs produced by the VIIRS Quarterly Surface Type (VQST) IP Unit. The other two IPs, the Gridded Biomes IP, and Gridded Annual Maximum and Minimum Monthly NDVI (GAMMMN) IP, are described in sections 4.3.4.7 and 4.3.4.8 respectively. In the previous delivery the VQST IP Unit was designed to also produce a Continuous Fields IP. The Continuous Fields IP is dropped in this version because it is not presently required by any units, and there is no existing code for producing this IP.

4.3.4.8 Gridded Biomes IP

The Gridded Biomes IP is another IP produced by the Quarterly Surface Type IP Unit. It contains the information on biome types required for deriving leaf area index (LAI) and fraction of absorbed photosynthetically active radiation (FPAR) (Myneni et al., 2002). These biome types include the following:

1. Grasses and cereal crops
2. Shrubs
3. Broadleaf crops
4. Savannas
5. Broadleaf forests
6. Needle forests
7. Urban
8. Non-vegetated lands

Unlike the GQST IP, the Gridded Biomes IP is not directly generated from the VIIRS monthly IPs using a classifier, but cross-walked from the IGBP types in the GQST IP using two additional ancillary data layers, with one being the second label as a byproduct of the MODIS land cover classification produced by Boston University, and the other describing the probability of the occurrence of broadleaf vegetation. The reader is referred to the VIIRS Surface Type ATBD *[Y2402]* for details on the cross-walking algorithm.

4.3.4.9 Gridded Annual Max and Min Monthly NDVI IP

This IP is required by the Surface Type EDR to calculate green vegetation fraction according to the work of Gutman and Ignatov (1998). It contains the maximum and minimum monthly NDVI values of the past 12 consecutive months, with the maximum NDVI value representing the NDVI value for surface with 100% green vegetation cover and the minimum NDVI value representing that for bare soil with 0% green vegetation cover. Note that for many land pixels their actual maximum and minimum NDVI values of the past 12 months do not correspond to 100% and 0% green vegetation fraction, because the actual green vegetation fraction value for these pixels may never reach 0% or 100% within any 12-month periods. Therefore for these pixels the calculated maximum and minimum NDVI values are hypothetical values, i.e., the would-be NDVI values assuming the green vegetation fraction could reach 100% and 0% during the past 12 months. For details on how the maximum and minimum NDVI values are calculated and how they are used to calculate green vegetation fraction, the reader is referred to the VIIRS Surface Type ATBD *[Y2402]*.

4.3.4.10 Gridded Snow/Ice Cover IP

The Gridded Snow/Ice Cover (GSIC) IP is used by the VIIRS Cloud Mask algorithm to set a snow/ice mask in the VIIRS Cloud Mask IP. The mask is needed by the VIIRS Cloud EDRs. For further details on the VIIRS Cloud Mask algorithm, the reader is directed to the VIIRS Cloud Mask ATBD *[Y2412]*

The structure of the GSIC IP is shown in Table 11.

Table 11. Gridded Snow/Ice Cover (GSIC) IP array structure.

Dimension	Elements
Global Grid (Spatial)	Grid Cell Row and Column Numbers
Parameters	Snow/Ice Mask, Observation Time, Geolocation Error (gGErr)

The GSIC IP is a running composite snow/ice mask. It is produced by a compositing method that retains the most recent Snow/Ice Cover of sufficient quality for each grid cell. Input data include the VIIRS Snow Cover EDR (used for Land pixels) and the VIIRS Ice Concentration IP (used for ocean or fresh water pixels.) For land pixels, each imagery resolution VIIRS pixel value for Snow Cover is mapped to a VIIRS grid cell. For the current implementation, the mapping is done by the nearest neighbor method (cf. Section 4.3.3.1). From the set of pixels mapped to a given grid cell, a subset is selected that meet the following criteria: 1) good quality, 2) pixel geolocation error less than the geolocation error currently stored in the grid cell OR time tag of the grid cell is older than a threshold time interval. If any pixel in the selected subset contains a snow classification in the snow binary map field of the EDR, the VIIRS grid cell is tagged as snow/ice covered. If all pixels in the selected subset contain a no snow classification in the snow binary map field of the EDR, the VIIRS grid cell is tagged as snow/ice free.

For ocean or fresh water pixels, the VIIRS Ice Concentration IP is examined. Each imagery resolution VIIRS pixel is mapped to a VIIRS grid cell. For the current implementation, the mapping is done by the nearest neighbor method (cf. Section 4.3.3.1). From the set of pixels mapped to a given grid cell, a subset is selected that meet the following criteria: 1) good quality, 2) pixel geolocation error less than the geolocation error currently stored in the grid cell OR time tag of the grid cell is older than a threshold time interval. If any pixel in the selected subset has an ice fraction and concentration weight greater than their threshold values (nominally 0.5) in the ice fraction and concentration weight fields of the IP, the VIIRS grid cell is tagged as snow/ice covered. If all pixels in the selected subset with concentration weight greater than the threshold value have ice fraction less than the threshold value (nominally 0.5), the VIIRS grid cell is tagged as snow/ice free.

For either snow-covered land or ice-covered water, the gridding algorithm also incorporates an ancillary snow/ice data set. If the time tag of the grid cell is older than the threshold time interval, but no pixel in the selected subset is of good quality, then the VIIRS grid cell is tagged as snow/ice covered or snow/ice free based on the corresponding grid cell in the ancillary snow/ice map. The GSIC IP grid cell is flagged as having been set by ancillary data. A grid cell which is flagged as having been set by ancillary data will continue to be updated by ancillary data until the conditions for setting the cell based on VIIRS data can again be satisfied. The grid contents are left unchanged if there are no VIIRS pixels in the selected subset for a given cell and the corresponding ancillary snow/ice data are unavailable.

At any time, the GSIC IP contains the best estimate of current Snow/Ice Cover, based on the most recent swath observations, or the most recent valid ancillary snow/ice estimate. The GSIC IP is used to set a snow/ice mask in the VIIRS Cloud Mask for subsequent swaths.

The IP is needed because the VIIRS snow and ice algorithms require the VIIRS Cloud Mask IP as input data. Therefore, the Cloud Mask algorithm cannot set its snow/ice mask from the output products of the VIIRS snow and ice algorithms.

It should be noted that the GSIC IP would not be needed if the VIIRS EDR processing architecture was revised so that the VIIRS Cloud algorithms were to obtain a snow/ice mask directly from the snow and ice algorithm output rather than from the Cloud Mask. This change would reduce snow/ice mask error and would reduce storage requirements, but would increase Cloud EDR latency.

4.3.4.11 Previous Ice Age IP

The Previous Ice Age (PIA) IP is required for the production of the VIIRS Sea Ice Characteristics EDR. It is used by the VIIRS Ice Age unit to classify identified ice reflectance and/or ice temperature modes as corresponding to first year ice or multi-year ice. Details on how this is done can be found in the Sea Ice Characterization ATBD *[Y2409]*.

The structure of the PIA IP is shown in Table 12.

Table 12. Previous Ice Age (PIA) IP array structure.

Dimension	Elements
Global Grid (Spatial)	Grid Cell Row and Column Numbers
Parameter	Ice Age (New/Young, First Year, Multi-year), Observing Time

The PIA IP is a running composite of Sea Ice Age. It is produced by a compositing method that retains the most recent Ice Age of sufficient quality for each grid cell.

The VIIRS Sea Ice Characteristics EDR is examined. This EDR contains ice age (new/young, first year, multi-year) reported for horizontal cells that are 3x3 aggregates of the imagery pixels. Each horizontal cell is mapped to a VIIRS grid cell. For the current implementation, the mapping is done by the nearest neighbor method (cf. Section 4.3.3.1). Each horizontal cell that maps to a given VIIRS grid cell is examined. If the horizontal cell is of good quality, is cloud-free, and has a pure ice age classification (new/young, first year, or multi-year) the VIIRS grid cell is tagged with that classification. The effect is to tag the grid cell with the classification of the good horizontal cell that is examined last. This is acceptable for the PIA IP, because the sea ice algorithm uses the IP to accumulate a statistical distribution of ice age types in the region. Therefore, even though the method for classifying the gridded ice age will bias a given grid cell with the age of the last horizontal cell examined for that grid cell, there is not expected to be a bias in the statistical distribution of ice age for all the grid cells in the region.

At any point, the PIA IP contains the current best estimate of Sea Ice Age. The PIA IP is used as input to the Sea Ice Characteristics EDR processing for subsequent swaths.

4.3.4.12 Other Gridded IPs

The Gridded BRDF Archetypal IP and the Gridded Surface Albedo IP are described in Y2398-SurfaceAlbedo-ATBD.doc and Y2483-VIIRS-LAND-Albedo-DDD.doc.

4.3.5 Re-gridding of Auxiliary Data

Auxiliary data will be processed for each VIIRS granule. After the receipt of a granule, a subset of the required auxiliary data will be extracted. This subset will cover the same spatial area as the granule. Resampling will be performed using a run-time selectable option of either nearest neighbor or bi-linear interpolation (for most data) for each pixel location within the granule. Interpolated values of the selected auxiliary data will be stored using the same indexes that identify pixels. EDR algorithms will have direct access to the auxiliary data that a pixel retrieval needs by using the same indexes that EDR algorithms use to access pixel data.

4.3.6 Re-gridding of Gridded VIIRS IPs

Some VIIRS gridded IPs need to be re-gridded to the VIIRS swath for use in EDR processing. Table 13 contains the list of gridded IPs that require re-gridding.

Table 13. Gridded IPs Requiring Re-gridding

IP Name
Gridded Monthly Non-Snow Reflectance IP
Gridded Surface Albedo IP
Gridded Quarterly Surface Types IP
Gridded Snow/Ice Cover IP
Gridded Previous Ice Age IP
Gridded Annual Max & Min Monthly NDVI IP

Re-gridding is performed by the nearest neighbor resampling technique for the Previous Ice Age IP and the Snow/Ice Cover IP. The Land products are regridded by the more complex and time-consuming area weighting technique. As an SDR becomes available, its geolocation fields can be used to map any of the gridded IPs back to the VIIRS swath. The newly produced swath based IP is then available for subsequent processing.

4.3.7 Compositing

Use of composited data instead of individual swaths acquired during any specific dates is a requirement common to most global land cover classification algorithms (e.g. DeFries et al., 1998; DeFries and Townshend, 1994; Friedl et al., 2002; Hansen et al., 2000; Loveland et al., 1991), because in order for the output classification to be globally consistent, the input images must be spatially contiguous and consistent. Due to extensive cloud cover over many parts of the Earth’s surface at any given time, however, the VIIRS instrument won’t be able to acquire spatially contiguous and cloud free data for the entire globe in any single date, though it is designed to scan the entire globe on a daily basis.

Compositing is a procedure for producing spatially contiguous and consistent images of the globe using observations accumulated over a predefined period. Week, 10-day, bi-week, and month are commonly used compositing periods. For the VIIRS Quarterly Surface Type IP algorithm the calendar month is selected as the compositing period, because most climate data records are collected at monthly intervals and decision making often requires monthly data. For areas with persistent cloud cover, a shorter compositing period could result in considerable residual cloud contamination in the composited products (Moody and Strahler, 1994).

The main goal of compositing is to select the pixels with least cloud contamination and atmospheric effect to construct a cloud-free, spatially contiguous image representing the compositing period. Cloud contamination and other atmospheric effects generally lower NDVI values, so a maximum NDVI would select the least cloud- and atmospheric-contaminated pixels. This method, called the maximum value compositing (MVC) method (Holben, 1986), generally works over near-Lambertian surfaces. But for non-Lambertian surface types, it tends to select off-nadir pixels with large, forward-scatter view angles (Goward et al., 1991; Moody and Strahler, 1994). Two methods are used to mitigate this problem. One is to constrain the view angle when more than one cloud free observations are available within the compositing period. This method, called controlled view angle MVC (CV-MVC), has been the major method for producing MODIS VI composites (Huete et al., 2002). The other method uses the cloud free observations to fit a BRDF model and derives the would-be nadir view observation assuming common illumination geometry based on the BRDF model (Schaaf et al., 2002). The BRDF models and nadir adjustment algorithms are detailed in the VIIRS Surface Albedo ATBD *[Y2398*]. As mentioned earlier, because the science community currently has mixed opinion on BRDF algorithms for operational applications, the BRDF based compositing method is available as an option.

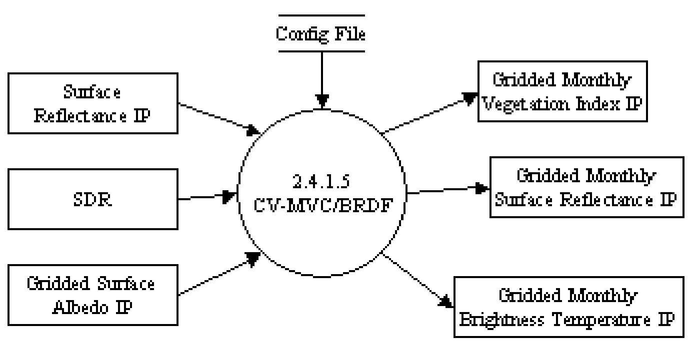

Figure 9. Overall data flow of the compositing procedure.

Figure 9 shows the overall structure of the compositing algorithm. Detailed steps of the two compositing methods are described below:

1. CV-MVC method

    a. Input bands include surface reflectance for all VIIRS moderate resolution bands except M6 and M9, gridded from every swath.

b. Outputs include a single "best" value within the compositing period for each of the input band plus NDVI.

c. The "best" observation means the one with least cloud contamination and closest to nadir view.

d. How to select the "best" observation within the compositing period

    i. A "good" observation is defined according to the QA flags of the gridded surface reflectance IP as:

        1. Cloud mask - confident clear
        2. Day/night - day
        3. Shadow detected - no shadow detected
        4. Heavy aerosol - no heavy aerosol

    ii. If there are more than one "good" observation,

        1. Calculate NDVI = (M7 – M5)/(M7 + M5) for all "good" observations

        2. Round the NDVI values to the second decimal point and select the highest and second highest NDVI values. If there are more than one observations with the same rounded NDVI values, select the one with the smallest viewing angle;

        3. Once the two observations with highest and second highest NDVI values are identified, if the difference in viewing angle is less than 5 degree between the two observations and the difference in NDVI value is greater than 0.01, the observation with higher NDVI value should be selected. Otherwise the one with the smaller view zenith angle should be selected;

    iii. If there is only one "good" observation, it is the "best";

    iv. If there is no "good" observation, the "best" observation is the one having highest NDVI value

e. Once the "best" observation within one month is identified, the values of different bands from this observation will be the composited values for the corresponding output bands. The NDVI calculated using M5 and M7 will be the monthly NDVI composite value.

2. BRDF based compositing procedure

   a. Inputs include nadir view reflectance for M1 – M5, M7, M8 and M10 – M11, and corresponding kernel_model_status flag. These inputs are calculated in the Gridded Surface Albedo Unit.

   b. For each compositing period, count the number *n* of the BRDF based estimates whose model inversion periods overlap the compositing period and whose kernel_model_status = 3. If

      i. *n* > 1, the composited value for each band is the average of the *n* observations weighted by overlapping length, i.e.,

$$\frac{\text{sum(band\_value} \times \text{\#\_overlapping\_days for the } n \text{ observations)}}{\text{sum(\#\_overlapping\_days for the } n \text{ observations)}}$$

      ii. *n* = 1, use this observation as the composited value

      iii. *n* = 0, use the CV-MVC compositing procedure as described above

   c. Composited NDVI will be calculated using the composited M5 and M7 values.

The reflective bands (M1 M1 – M5, M7, M8 and M10 – M11) and NDVI can be composited using either the BRDF based compositing procedure or the CV-MVC method (if the BRDF based compositing procedure is turned off, or BRDF model fitting is unsuccessful due to lack of sufficient information). However, The BRDF based compositing procedure does not apply to the thermal bands (M12 – M16). Therefore, the thermal bands are always composited using the CV-MVC method.

GMVI, GMSR, and GMBT are calculated in a running fashion, maintaining the "best estimate" for VI, surface reflectance, and brightness temperature according to the CV-MVC criterion, which is described in section 4.3.7. Granules are added individually, and at the end of a month, the GMVI, GMSR, and GMBT contain the best estimates for the month. One then begins anew for the following month.

If BRDF processing is used, then after these CV-MVC-based monthly IPs are completed, the values are BRDF adjusted using coincident data from the Gridded Surface Albedo IP according to the BRDF algorithm. The aim of the BRDF algorithm is to replace the CV-MVC "best estimate" with a derived nadir measurement based on a BRDF model fitted to qualified directional VIIRS observations.

5.0 Practical Considerations

5.1 NUMERICAL COMPUTATION CONSIDERATIONS

Re-gridding and gridding occur in distinctly different processing environments and therefore have different timing requirements.

Gridding is a post-processing function and is therefore not driven by EDR latency requirements. The driver for gridding is the need to have updated gridded products on a timely basis. The update time depends on the specific product. Ideally, Gridded IPs that contains most recent properties (e.g. Previous Snow/Ice Cover IP) would be updated before the next VIIRS observation of the same region. For NPP, the time until the next observation can be as short as the orbital period (~ 100 minutes). For the NPOESS system, the time will be much shorter.

Re-gridding occurs between SDR production and EDR production. Its timing is therefore driven by the latency requirements of its customer EDRs. It is important that re-gridding methods not be too computationally intensive.

6.0 REFERENCES

Bracewell, R.N., “Two Dimensional Imaging”, p 247, 1995.

DeFries, R. S., Hansen, M., Townshend, J. R. G., and Sohlberg, R., 1998, Global land cover classifications at 8km spatial resolution: the use of training data derived from Landsat imagery in decision tree classifiers, *International Journal of Remote Sensing*, **19**(16): 3141-3168.

DeFries, R. S., and Townshend, J. R. G., 1994, NDVI-derived land cover classifications at a global scale, *International Journal of Remote Sensing*, **15**(17): 3567-3586.

Friedl, M. A., Zhang, X. Y., Muchoney, D., Strahler, A. H., Woodcock, C. E., Gopal, S., Schneider, A., Cooper, A., Baccini, A., Gao, F., Schaaf, C., McIver, D. K., and Hodges, J. C. F., 2002, Global land cover mapping from MODIS: Algorithms and early results, *Remote Sensing of Environment*, **83**(1-2): 287-302.

Goward, S. N., Markham, B., Dye, D. G., Dulaney, W., and Yang, J., 1991, Normalized difference vegetation index measurements from the Advanced Very High Resolution Radiometer, *Remote Sensing of Environment*, **35**: 257-277.

Gutman, G., and Ignatov, A., 1998, The derivation of the green vegetation fraction from NOAA/AVHRR data for use in numerical weather prediction models, *International Journal of Remote Sensing*, **19**(8): 1533-1543.

Hansen, M., DeFries, R. S., Townshend, J. R. G., and Sohlberg, R., 2000, Global land cover classification at 1 km spatial resolution using a classification tree approach, *International Journal of Remote Sensing*, **21**(6/7): 1331-1364.

Holben, B. N., 1986, Characteristics of maximum-value composite images from temporal AVHRR data, *International Journal of Remote Sensing*, **7**(11): 1417-1434.

Huete, A., Didan, K., Miura, T., Rodriguez, E. P., Gao, X., and Ferreira, L. G., 2002, Overview of the radiometric and biophysical performance of the MODIS vegetation indices, *Remote Sensing of Environment*, **83**(1-2): 195-213.

Loveland, T. R., Merchant, J. W., Ohlen, D. O., and Brown, J. F., 1991, Development of a land-cover characteristics database for the conterminous US, *Photogrammetric Engineering and Remote Sensing*, **57**(11): 1453-1463.

Moody, A., and Strahler, A. H., 1994, Characteristics of composited AVHRR data and problems in their classification, *International Journal of Remote Sensing*, **15**(17): 3473-3493.

Myneni, R. B., Hoffman, S., Knyazikhin, Y., Privette, J. L., Glassy, J., Tian, Y., Wang, Y., Song, X., Zhang, Y., Smith, G. R., Lotsch, A., Friedl, M., Morisette, J. T., Votava, P., Nemani, R. R., and Running, S. W., 2002, Global products of vegetation leaf area and fraction absorbed PAR from year one of MODIS data, *Remote Sensing of Environment*, **83**(1-2): 214-231.

Quinlan, J. R., 1993, C4.5 programs for machine learning, The Morgan Kaufmann Series in Machine Learning, Morgan Kaufmann Publishers, San Mateo, California, 302 pp.

Reichenbach, S.E., Geng, F., Two-Dimensional Cubic Convolution, IEEE Transactions on Image Processing, Vol. 12, No. 8, August 2003, pp857-865.

Schaaf, C. B., Gao, F., Strahler, A. H., Lucht, W., Li, X., Tsang, T., Strugnell, N. C., Zhang, X., Jin, Y., Muller, J.-P., Lewis, P., Barnsley, M., Hobson, P., Disney, M., Roberts, G., Dunderdale, M., Doll, C., d'Entremont, R. P., Hu, B., Liang, S., Privette, J. L., and Roy, D., 2002, First operational BRDF, albedo nadir reflectance products from MODIS, *Remote Sensing of Environment*, **83**(1-2): 135-148.

Strahler, A.H., J-P. Muller (1996), MODIS BRDF/Albedo Product: Algorithm Theoretical Basis Document , http://eospso.gsfc.nasa.gov/ftp_ATBD/REVIEW/MODIS/ATBD-MOD-09/atbd-mod-09.pdf

Yang, K., Wolfe, R.E. MODIS Level 2 Grid with ISIN Map Projection.